Asian Journal of Chemistry; Vol. 30, No. 7 (2018), 1537-1545

ASIAN JOURNAL OF CHEMISTRY

https://doi.org/10.14233/ajchem.2018.21222

Synthesis, Characterization and Biological Activities of Some Metal Complexes Derived from Azo Dye Ligand 2-[2'-(5-Methyl thiazolyl)azo]-5-dimethylamino Benzoic Acid

KHALID J. AL-ADILEE* and SUDAD A. JABER

Department of Chemistry, College of Education, University of Al-Qadisiyah, Diwaniya 1753, Iraq

*Corresponding author: E-mail: khalidke_1962@yahoo.com; Khalid.Jawad@qu.edu.iq

Received: 11 January 2018; *Accepted*: 18 April 2018; *Published online*: 31 May 2018; AJC-18927

In this paper we report the synthesis and identification of Ni(II), Cu(II) and Zn(II) complexes with new thiazole based azo dye 2-[2'-(5-methyl thiazolyl)azo]-5-dimethyl amino benzoic acid (5-MeTAMB) by the diazotization of 2-amino-5-methyl thiazole and coupling with 3-dimethyl amino benzoic acid in alkaline alcoholic solution. The structures of the azo dye ligand and its metal complexes were confirmed by various analytical techniques like by elemental analysis (C.H.N.S), UV-visible, FT-IR spectroscopic, mass spectroscopic, ^{1}H NMR spectroscopic, SEM, XRD data and thermal studies (TGA & DSC). The magnetic moment value of metal complexes [ML_2] M = Ni(II) and Cu(II) occurs in the range of high spin octahedral environment of azo ligand while Zn(II) complex show diamagnetic properties and octahedral structure. The analytical and spectral techniques show that the ligand coordinates as tridentate (N,N,O) donor molecule. The antibacterial and antifungal activity of the thiazolylazo ligand and its metal complexes have shown activity towards both bacterial and fungal strains. The biological activity was also conducted by cells cytotoxicity and viability of the ligand and Cu(II)-complex was screened for *in vitro*, antitumor activity against human breast cancer using MTT assay. The results shows that this type of compounds plays an important role in the rate of inhibition of the growth of cells of cancerous and natural lines and indicate undoubtedly the possibility of using them as antitumor drugs against breast cancer.

Keywords: Synthesis, Thiazolylazo dye, Metal complexes, Spectral studies, Biological activity, Anticancerous.

INTRODUCTION

Thiazolylazo dyes are an important class of organic complexion compounds and very important class of chemical constituents having a wide applications in different fields such as leather, polymer, paint and coating industries as dyeing agent [1-3]. The dyeing capability of dye depends on functional groups present in the dyes, such as azo, hydroxyl, carboxylic acids, esters and amines [4,5]. The thiazolylazo dyes and its derivatives are also used for colouring consumer goods, such as clothes, plastics, textiles, food, toys and cosmetics [6,7]. Thiazolylazo dyes were also used in chemical operations such as spectrophotometry, solid phase extraction, liquid chromatography, electrochemistry and cloud point [8-10]. The application of thiazolylazo dyes in spectrophotometry is based on coloured compounds resulting from their reaction with metal ions, especially transition metals [10]. Thiazolylazo derivatives are active biological agents [11] which possess strong biological activities such as antihistamines [12], antitumor [13], anti-inflammatory [14], antibacterial effects [15] and production of drugs in chemotherapy [16].

Thiazolylazo compounds and some of its metal complexes also show significant effects against cancer and also exhibit microbial activities such as antibacterial [17], antiviral [18] and antifungal [19]. In this work describe the preparation and characterization of new thiazolylazo ligand (5-MeTAMB) and its complexes with Ni(II), Cu(II) and Zn(II) ions, is described biological activities (antibacterial and antifungal). The thiazolylazo ligand and its Cu(II) complex evaluated for *in vitro* anticancer activity against human breast cancer MCF7 by MTT assay.

EXPERIMENTAL

All the chemicals and solvents were of the highest purity obtained from BDH, Aldrich, sigma and Merck. Mass spectra was obtained using a Shimadzu Agilent Technologies 5973C at 70^e and MSD energy using a direct insertion probe (Acq method 10 W energy) at temperature 90-110 °C. ^{1}H NMR spectra were recorded in DMSO on a Bruker 500 MHZ spectrophotometer using TMS as an interior reference. IR spectra of the ligand as well as the complexes are recorded as KBr discs using a Shimadzu 8400 S FT-IR spectrophotometer in wave number at range (4000-400) cm^{-1}. The electronic spectra of ligand and its metal complexes were recorded on a T80-PG double beam UV-visible spectrophotometer in the range of

(200-1100) nm in absolute ethanol (10^{-4} M) solution. Elemental analysis (C.H.N.S) was performed on a Euro EA 1106 elemental analyzer. The metal contents of the complexes were measured using atomic absorption technique by Shimadzu AA-6300. Magnetic susceptibility measurements of the metal complexes in powder form were carried out on Balance Magnetic (MSB-MKI) apparatus. Molar conductivity measurements were made with DMSO solution (10^{-3} M) at room temperature using a31A digital conductivity meter. Melting point apparatus melting point, SMP, Stuart. pH measurements are carried out using Philips pw 9421 pH meter (pH ± 0.001). X-ray diffraction were measured by using a Shimadzu X-ray diffractometer (XRD 600). TGA analysis were recorded PL-TG using Perkin Elmer TGA-4000. Scanning electron microscopy (SEM) images of ligand and its metal complexes were taken using micrograph ZEISS EM3200.

Synthesis of azo dye ligand (5-MeTAMB): The new thiazolylazo dye ligand has been synthesized by the diazotization coupling reaction (**Scheme-I**) by Al-Adilee [20] and Fan *et al.* [21] method with some modification. 2-Amino-5-methyl thiazole (1.14 g, 0.01 mol) was dissolved in mixture 5 mL of formic acid and 7 mL of concentrated sulfuric acid, then 16 mL distilled water were added. To this solution was added drop-wise a solution of 0.80 g (0.012 mol) of sodium nitrite ($NaNO_2$) in 35 mL distilled water at (0-5) °C and the mixture was stirred for 30 min at (0-5) °C. The resulting diazonium solution was added drop-wise with cooling and stirring continuously at (0-5) °C in to beaker (500 mL) containing 1.65 g (0.01 mol) of 3-dimethyl amino benzoic acid was dissolved in 10 mL of pyridine and 30 mL of methanol and cooled to (0-5) °C. The mixture was stirred for 2 h in an ice-bath and allowed to stand overnight. The precipitate formed was filtered off and first purified by the base-acid recrystallized method and further purified by recrystallization from DMF-water (1:1). A dark purplish crystals, which decomposes at 198 °C, was obtained in a yield of about 83 %. The purity was confirmed by the element analysis and TLC techniques. Its structure was verified by ^{1}H NMR, mass spectrum, IR and UV-visible spectrometry.

General method for the preparation of metal complexes: The metal complexes were prepared using corresponding metal chlorides and the ligand (5-MeTAMB) amount of 0.580 g (0.002 mol) from ligand, dissolved in 50 mL of absolute ethanol was gradually added with stirring a stoichiometric to (0.001 mol) amount of [1:2] M:L for Ni(II), Cu(II) and Zn(II) chloride salt dissolved in 40 mL hot buffer solution (ammonium acetate) at pH = 7.0. The mixture was heated to (50-70) °C at 50 min, then left over night. The separated solid complexes were filtered off, washed with distilled water and little warm ethanol to remove any traces of unreacted materials. The complexes obtained were finally dried under vacuum desiccators over combined $CaCl_2$. The analytical and physical data of ligand and its metal complexes are collected in Table-1.

RESULTS AND DISCUSSION

Physical and chemical properties of azo dye (5-MeTAMB): The thiazolylazo dye ligand is a dark purplish crystals sparingly soluble in water. It is soluble in methanol, acetone, ethanol and chloroform but easily soluble in DMSO, DMF and alkaline aqueous solutions and strongly acidic solutions. It is yellow-reddish in strongly acidic solution, dark purple in neutral and violet-bluish in strongly alkaline solution. The equilibrium of the dissociation can be written as shown (**Scheme-II**), the dissociation constants were evaluated by a spectrophotometric method [22].

Metal:ligand ratio: The composition of metal complexes were investigated spectrophotometrically by mole ratio method at fixed concentration and wavelength of maximum absorption (λ_{max}) of metal ion and increasing amount of ligand solutions (0.25 mL each add up 3 mL). The colour solutions of metal complexes increase the intensity, ratio [M:L] and the continued stability of colour after the point of intersection indicating the composition of the metal complexes. The molar ratios [M:L] suggested for the formation of each metal complexes are [1:2] [23].

Molar conductivity measurements: The molar conductance of prepared metal complexes are shown in Table-2,

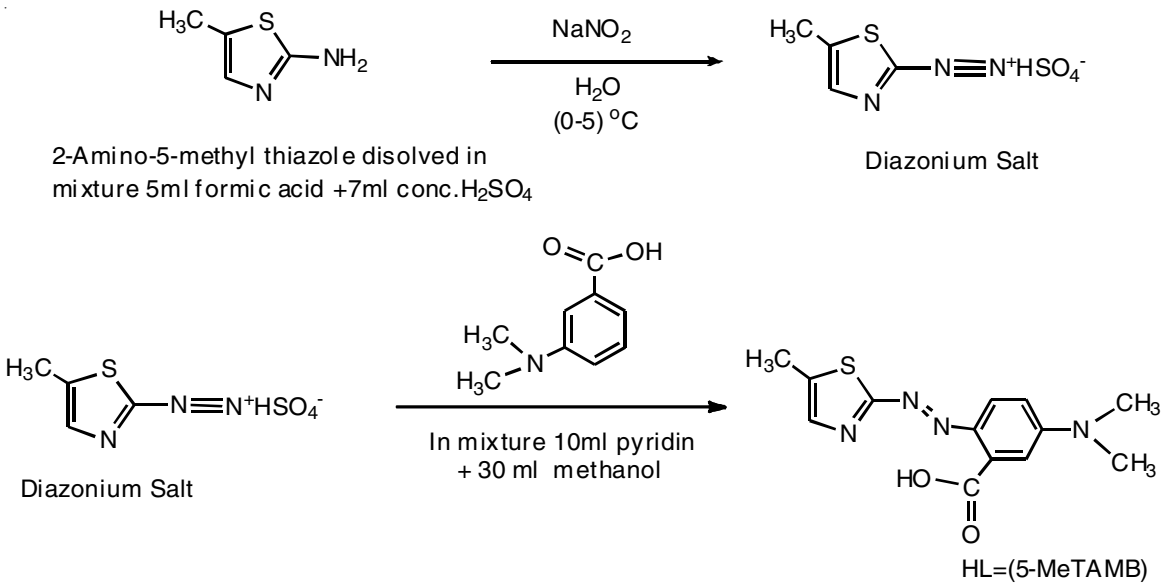

Scheme-I: Synthesis of ligand (5-MeTAMB)

TABLE-1
PHYSICAL PROPERTIES AND ELEMENTAL ANALYSIS FOR LIGAND (5-MeTAMB) AND ITS METAL COMPLEXES

Compd.	Colour	m.p. (°C)	Yield (%)	m.f. (m.w.)	Elemental analysis (%): Found (calcd.)				
					C	H	N	S	M
5-MeTAMB (L)	Dark purplish	198	83	$C_{13}H_{14}N_4O_2S$ (290.34)	54.31 (53.77)	4.95 (4.86)	19.16 (19.29)	11.22 (11.04)	–
$[Ni(L)_2]\cdot H_2O$	Greenish blue	240	79	$C_{26}H_{28}N_8O_5S_2Ni$ (655.37)	48.12 (47.64)	4.05 (4.03)	17.38 (17.09)	10.05 (9.78)	9.17 (8.95)
$[Cu(L)_2]\cdot H_2O$	Blue	231	77	$C_{26}H_{28}N_8O_5S_2Cu$ (660.22)	47.81 (47.29)	4.02 (4.27)	17.35 (16.97)	10.17 (9.71)	9.81 (9.62)
$[Zn(L)_2]\cdot H_2O$	Violet	243	69	$C_{26}H_{28}N_8O_5S_2Zn$ (662.09)	47.35 (47.16)	4.32 (4.26)	17.28 (16.92)	9.49 (9.68)	10.18 (9.87)

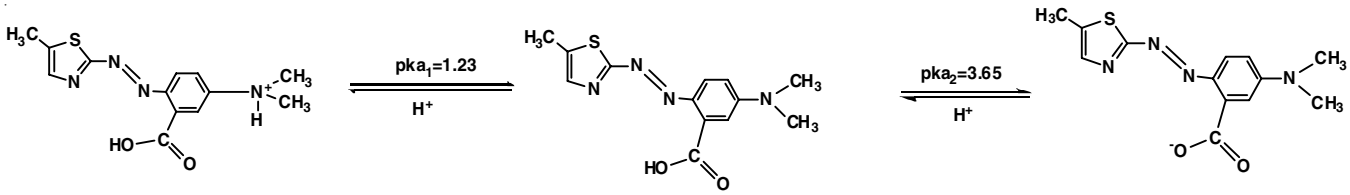

pH ≤ 2.5; [LH_2^+] protonated form, yellow-reddish
λ_{max} = 468 nm
(ε) = 1.28 × 10^3 L mol^{-1} cm^{-1}

pH = 4.0-7.0; [LH] neutral form, purple
λ_{max} = 440 nm
(ε) = 9.7 × 10^3 L mol^{-1} cm^{-1}

pH = 7.5-9.5; [L^-] anion form, violet
λ_{max} = 567 nm
(ε) = 2.37 × 10^3 L mol^{-1} cm^{-1}

Scheme-II: Equilibrium of the dissociation of thiazolylazo dye ligand (5-MeTAMB)

TABLE-2
OPTIMAL CONCENTRATION, MAXIMUM WAVELENGTH (λ_{max}), MOLAR ABSORPTIVITY (ε), STABILITY CONSTANTS VALUES (β AND log β) AND MOLAR CONDUCTIVITY OF METAL COMPLEXES

5-MeTAMB	Metal ion	Optimal conc. × 10^{-4} M	λ_{max} (nm)	ε × 10^3 (L mol^{-1} cm^{-1})	β (L^2 mol^{-2})	log β	Molar conductance (S cm^{-1} mol^{-1})
λ_{max} = 440 nm	Ni(II)	1.50	625	19.68	1.527 × 10^{12}	12.181	10.27
ε = 9.7 × 10^3 L mol^{-1} cm^{-1}	Cu(II)	1.75	527	34.28	7.049 × 10^{10}	10.894	9.03
Conc. = 1.50 × 10^{-4} M	Zn(II)	1.25	608	11.01	2.185 × 10^{11}	11.339	13.28

carried out in DMF (10^{-3}) at room temperature. The values of conductivity indicated that the metal complexes of Ni(II), Cu(II) and Zn(II) ions are non-electrolytes in nature [24].

Calculation stability constants (β): Stability constants (β) values of metal complexes are obtained spectrophotometrically by measuring the absorbance of solution of the ligand and metal ion solution at fixed wavelength (λ_{max}) and optimum concentration at pH = 7.0. The degree of formation of the metal complexes are obtained by the relationship, $\beta = (1-\alpha)/4\alpha^3c^2$ and $\alpha = A_m-A_s/A_m$, where A_m and A_s are the absorbance of fully and partially formed metal complex respectively at optimum concentration [25]. The stability constants of metal complexes values for the preparation of metal complexes are listed in the Table-2. The stability constants of metal complexes according to the following sequence: Ni(II) > Cu(II) > Zn(II). The sequence of metal ions of the first row transition metal agree with Irving-Williams series of stability constant [26].

^{1}H NMR spectra: The ^{1}H NMR spectra of thiazolylazo dye ligand (5-MeTAMB) and Zn(II) complex [27] was measured in DMSO-d_6 as solvent with TMS as an internal reference (500 MHz). This compounds have been studied and listed in Table-3.

Infrared spectral studies: IR spectral data of the prepared thiazolylazo dye ligand (5-MeTAMB) and its metal complexes with Ni(II), Cu(II) and Zn(II) ions are presented in Table-4. The shifts in the position or change in the shape of the metal complexes bands compared with those absorption bands of free ligand due to the formation of the metal complexes bands

TABLE-3
^{1}H NMR SPECTRA OF THIAZOLYLAZO DYE LIGAND (5-MTAMB) AND ITS Zn(II) COMPLEX

Ligand (5-MeTAMB) δ, ppm (H atoms, peak, assignment)	*J-J* coupling	Zn(II) complex δ, ppm (H atoms, peak, assignment)	*J-J* coupling
2.444 (DMSO-d_6)	5.984	2.984 (DMSO-d_6)	31.113
2.896 (6H, S, 16, 17)	11.218	3.052 (6H, S, 6, 25)	15.567
3.437 (3H, S, 6)	6.148	3.523 (12H, S, 16, 17, 36, 37)	31.563
7.089-7.135 (1H, d, 13)	2.168	5.384 (2H, S, H_2O)	6.557
7.252-7.277 (1H, d, 14)	2.222	6.917 (2H, S, 4, 24)	5.952
7.367 (1H, S, 4)	2.292	7.106-7.136 (2H, d, 13, 32)	5.000
7.653 (1H, S, 11)	2.790	7.171 (2H, S, 11, 30)	5.391
10.675 (1H, S, 19)	2.062	8.084-8.197 (2H, d, 14, 33)	5.567

TABLE-4
KEY IR (cm^{-1}) BANDS OF THIAZOLYLAZO DYE LIGAND (5-MeTAMB) AND ITS METAL COMPLEXES

$[Zn(L)_2]\cdot H_2O$	$[Cu(L)_2]\cdot H_2O$	$[Ni(L)_2]\cdot H_2O$	Ligand (LH)	Group
3445 m,br (H_2O)	3447 m (H_2O)	3418 m,br (H_2O)	3458 m	-COOH
3192 m,br	3348 s	3368 w	3073 m	ν(C-H) Ar-ring
2924 w	2924 w	3102 w	2924 m	ν(-CH_3)
2859 s	2850 w	2926 s	2884 w	ν$N(CH_3)_2$
1649 m	1651 m	1651 m	1713 m	ν(C=O)
1599 m,sh	1595 s	1595 s	1600 w	ν(C=N)
1524 s	1524 s	1526 m	1560 s	ν(N=N)
1398 m	1391 m	1394 s	1388 w	Ar-ring
823 w	846 w	864 w	765 m	
1451 m	1452 w	1395 s	–	ν(COO^-) asym.
1398 s	1391 m	1394 s	–	ν(COO^-) sym.
615 w	596 w	605 w	–	M-O
519 w	515 w	521 w	–	M-N

of free ligand. Depend on IR spectral data lead to suggest that ligand (5-MeTAMB) behaves as a tridentate chelating agent coordinating with metal ions by a carboxylic oxygen, azo nitrogen which is the farthest of thiazole ring and nitrogen atom in thiazole ring to forming two five membered chelating ring [28].

Mass spectra: The mass spectrum of thiazolylazo dye ligand (5-MeTAMB) showed a molecular ion peak M^+ at m/z^+ = 290.30 attributed to the original molecular weight of ligand (290.34) (Fig. 1). The mass spectrum of Cu(II) complex showed a molecular ion peak M^+ at m/z^+ = 660.21, equivalent to its molecular weight supporting the suggested structure for Cu(II) complex (Fig. 2). The result of the expected mass fragmentation have shown that they correspond to mass spectra of the ligand (5-MeTAMB) and its Cu(II) complex [29].

Electronic spectra and magnetic susceptibility measurements: The electronic absorption spectra of ligand (5-MeTAMB) and its metal complexes with Ni(II), Cu(II) and Zn(II) ions were recorded in freshly prepared absolute ethanol solution

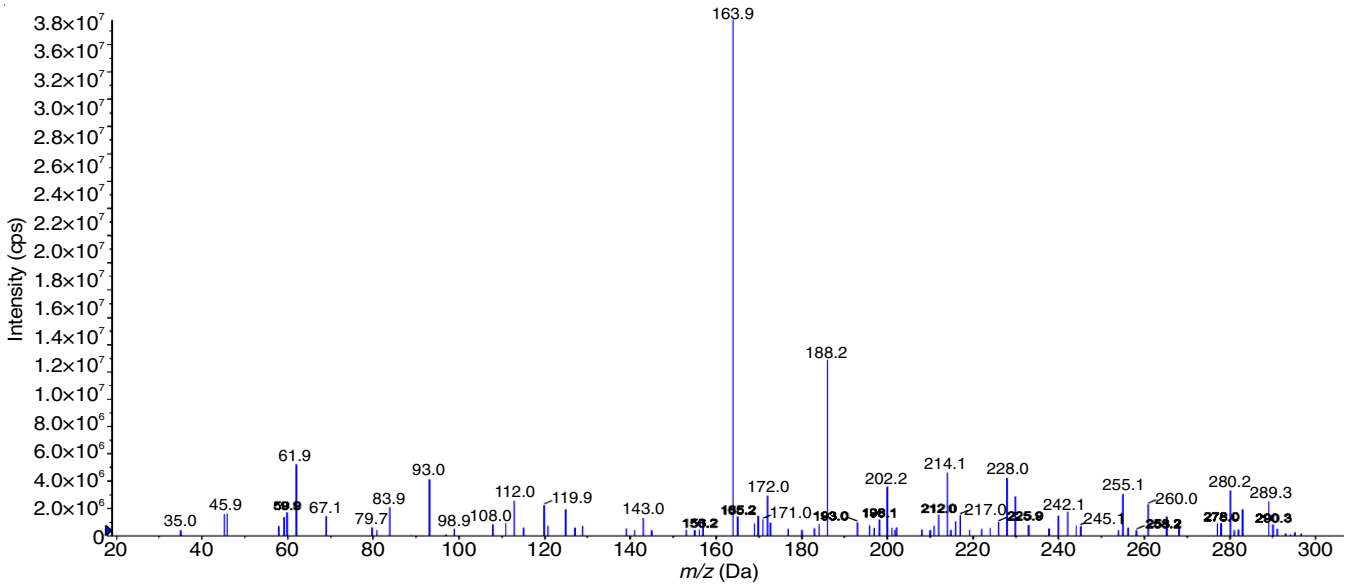

Fig. 1. Mass spectrum of thiazolylazo dye ligand (5-MTAMB)

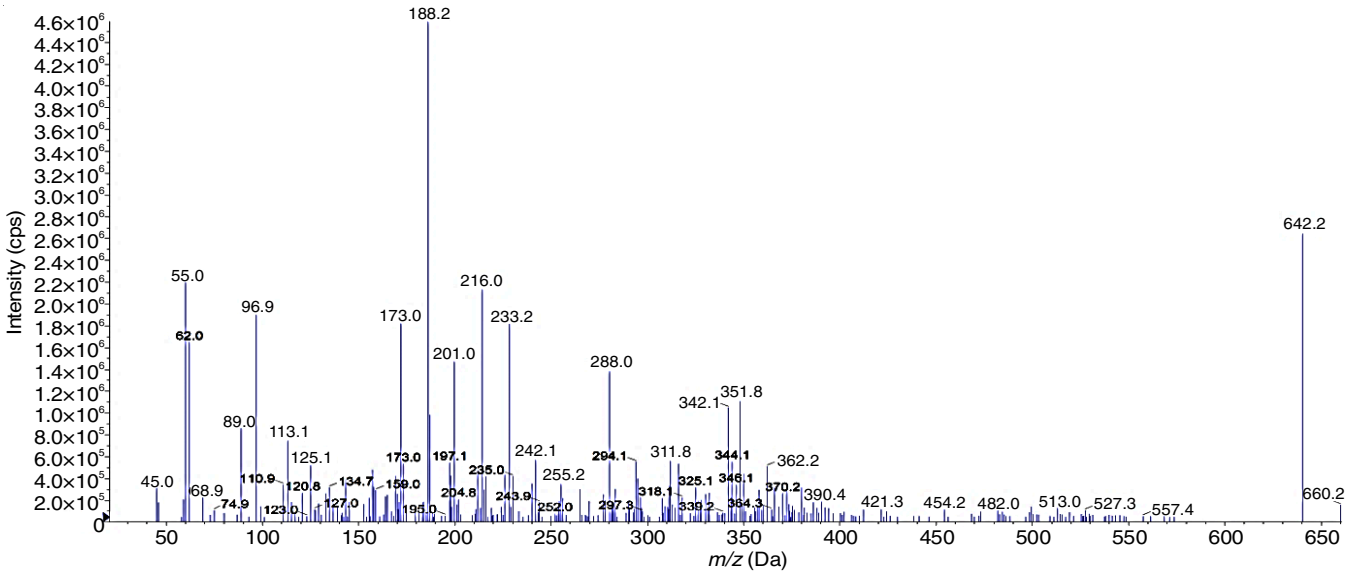

Fig. 2. Mass spectrum of Cu(II) complex; $[Cu(L)_2]\cdot H_2O$

(10^{-3} M) at room temperature. The spectral data and electronic transitions (nm, cm^{-1}) are presented in Table-5. The electronic spectrum of free ligand show three absorption bands at 250 nm (40000 cm^{-1}), 295 nm (33898 cm^{-1}) and 440 nm (22727 cm^{-1}).

The first band can be due to a $\pi\rightarrow\pi^*$ transition in thiazole ring [25], while the second band assigned to $\pi\rightarrow\pi^*$of the two interact (C=C) group of atomic of aromatic and thiazole ring and third band due to $n\rightarrow\pi^*$ of the azo group (-N=N-). This band was shown at a red shift on coordination with a metal ions [23].

The electronic spectrum of the Ni(II) complex displayed bands at 856 nm (11682 cm^{-1}), 625 nm (16000 cm^{-1}) and 392 nm (25510 cm^{-1}). These three bands are attributed to $^3A_2g\rightarrow{}^3T_2g$ (ν_1), $^3A_2g\rightarrow{}^3T_1g_{(F)}$ (ν_2) and $^3A_2g\rightarrow{}^3T_1g_{(p)}$ (ν_3) transitions respectively in octahedral structure [30]. The Cu(II) complex exhibited a single broad band around at 527 nm (18975 cm^{-1}). The broadness band indicates the three transitions $^2B_1g\rightarrow{}^2A_1g$ (ν_1), $^2B_1g\rightarrow{}^2B_2g$ (ν_2) and $^2B_1g\rightarrow{}^2Eg$ (ν_3), which are of similar energy and give rise to only one broad absorption band ($^2B_1g\rightarrow{}^2Eg$) and suggest distortion octahedral geometry of the Cu(II) complex [31,32].

The electronic absorption spectrum of the Zn(II) complex did not show any *d-d* transition because of saturation with electrons (d^{10}). The Zn(II) complex exhibited one absorption band at 608 nm (16447 cm^{-1}) assignable to charge transfer [$d\pi(Zn^{2+})\rightarrow\pi^*$(HL)] transition where π^* (HL = 5-MeTAMB) was believed to be primarily dominated by the LUMO of the azo imine chromosphere [33]. UV-Visible spectra of the ligand and its metal complexes are shown in Fig. 3.

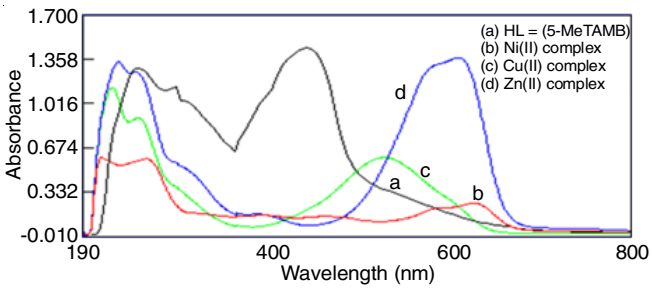

Fig. 3. UV-visible spectra of ligand (5-MeTAMB) and its metal complexes with Ni(II), Cu(II) and Zn(II) ions

Magnetic susceptibility studies: The magnetic moments obtained at room temperature for Ni(II) and Cu(II) complexes are listed in Table-5. The Ni(II) complex exhibited the magnetic moment value of 2.94 B.M. because of the presence of two unpaired electrons which indicates an a regular octahedral geometry ($t_2g^6\ eg^2$) high spin and sp^3d^2 hybridization [34]. The Cu(II) complex showed the magnetic moment value 1.78 B.M. due to the presence of one unpaired electron which may suggest a distorted octahedral geometry ($t_2g^6eg^3$) and sp^3d^2 hybridization [38]. The magnetic moment for Zn(II) complex shows a diamagnetic behaviour as it is diamagnetic complex with d^{10} configuration ($t_2g^6\ eg^4$) and sp^3d^2 hybridization [35].

Thermogravimetric analysis: Thermogravimetry (TG) is a technique in which the change in mass of the sample is determined as a function of time or temperature. Among all the methods, TG is the most widely used one. From TG curve, information related to the thermal stabilities, composition of the initial sample. The middle case compounds that are formed and in the final residue could be obtained [36]. The differential scanning calorimetric (DSC) and thermogravimetric analyses (TGA) curves for the ligand HL and its metal complexes are presented in Fig. 4, Table-6 illustrates the thermal analyses curves of the of ligand (5-MeTAMB) and its M(II) complexes.

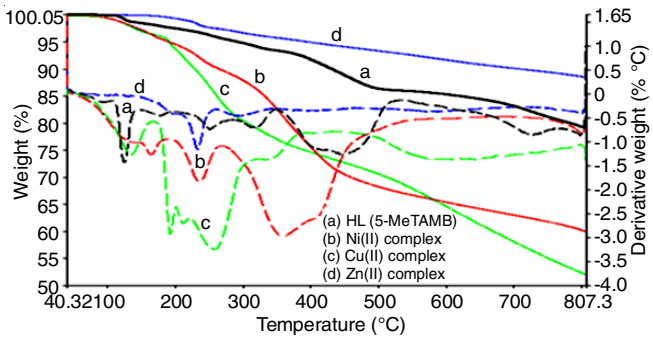

Fig. 4. Thermal analysis (TGA and DSC) of ligand (5-MeTAMB) and its M(II) complexes

Powder X-ray diffraction: Crystallinity and crystal phases of the as-synthesized ligand (5-MeTAMB) and its metal complexes nanoparticles were analyzed. The (XRD) patterns of ligand and complexes are shown in Fig. 5. The XRD of ligand and its complexes were recorded in the range of 5-80° (2θ) value, arising from diffraction of X-ray by planes of complex. The interplanar spacing (d) has been calculated from the position of intense peak using Bragg's equation: $\eta\lambda = 2d \sin\theta$, where λ = wavelength of X-ray used (CuK_α = 1.54A), η is an integer (1, 2, 3, 4 …), θ is the diffraction angle [37]. The 2θ values for the prominent peaks and the calculated spacing together with relative intensities with respect to most intense

TABLE-5
ELECTRONIC SPECTRA (nm AND cm^{-1}); MAGNETIC MOMENTS; PROPOSED GEOMETRY AND HYBRIDIZATION OF PREPARED METAL COMPLEXES

Compounds	λ_{max} (nm)	Absorption bands (cm^{-1})	Transitions	μ_{eff} (B.M.)	Geometry	Hybridization
HL	440	22727	$\pi\rightarrow\pi^*$	–	–	–
	295	33898	$n\rightarrow\pi^*$			
	250	116000	$n\rightarrow\pi^*$			
Ni(II) complex	856	11682	$^3A_2g\rightarrow{}^3T_2g_{(F)}$ (ν_1)	2.94	Octahedral (regular)	sp^3d^2 (high spin)
	625	16000	$^3A_2g\rightarrow{}^3T_1g_{(F)}$ (ν_2)			
	392	25510	$^3A_2g\rightarrow{}^3T_1g_{(P)}$ (ν_3)			
Cu(II) complex	527	18975	$^2B_1g\rightarrow{}^2Eg$	1.78	Octahedral (distorted)	sp^3d^2
Zn(II) complex	608	16447	$d\pi(Zn)^{2+}\rightarrow\pi^*$(HL)	Diamag.	Octahedral (regular)	sp^3d^2

TABLE-6
THERMAL ANALYTICAL RESULTS (TGA, DSC) OF LIGAND (5-MeTAMB) AND ITS METAL(II) COMPLEXES

Compound	TGA range (°C)	Mass loss (%) Estimated (calcd.)	Probable assignments	DSC
5-MeTAMB	120-202	3.06 (2.88)	Loss of dimethyl amine group	(+) 450
	202-528	20.60 (19.41)	Evolution CH_4, CO_2 gases	
$[Ni(L)_2]\cdot H_2O$	98-271	9.50 (10.33)	Loss H_2Omolecule and liberation N_2O gas.	(-) 270
	271-464	20.62 (19.88)	Evolution CH_4, CO_2 gases and formation of NiO	
$[Cu(L)_2]\cdot H_2O$	80-100	2.73 (3.49)	Loss H_2Omolecule	
	130-171	20.60 (21.21)	Loss of *N*,*N*-dimethyl aniline group	(-) 170
	171-390	22.30 (23.00)	Evolution CH_4, CO_2 gases and formation of CuO	(+) 213
$[Zn(L)_2]\cdot H_2O$	150-263	2.71 (2.55)	Loss H_2Omolecule	
	263-412	6.21 (6.27)	Liberation N_2O gas	(+) 296

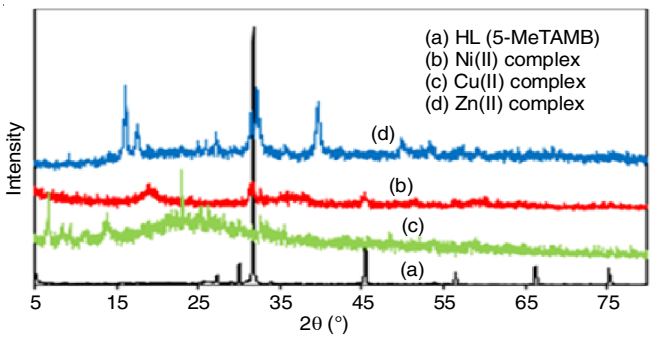

Fig. 5. Powder X-ray diffraction data of ligand (5-MeTAMB) and its M(II) complexes

peak have been listed in Table-7. The crystallite size is calculated using Debye-Scherrer equation [38]:

$$D_p = \frac{0.94\lambda}{\beta_{1/2}\cos\theta}$$

where D_p = average crystallite size, β = line broadening at half the maximum intensity in radians, θ = Bragg angle, λ = X-ray wavelength.

SEM analysis: Scanning electron microscopy (SEM) of the ligand (5-MeTAMB) and its metal complexes studies the surface morphology and state of the particles and accumulation, in addition to the distribution of these particles. The SEM image of ligand and metal complexes have been represented in Fig. 6.

SEM image shows the ligand (5-MeTAMB) have form of spherical shape with average size 73 nm with a ratio of less than aggregation. The SEM complexes showed that the particles are agglomerated and non-uniform particles are observed in some cases. Moreover, SEM micrographs (Fig. 6) of the metal complexes revealed that the surface morphology of metal complexes is changed by changing the metal ions [39]. The calculations of particles size were performed utilizing Menisci software.

The analysis of SEM for Ni(II) complex appeared in the form of a small particle size is heterogeneous surface and the average particle size of 103 nm, either the analysis of SEM for Cu(II) appeared in the form of heterogeneous surface and the average particle size 139 nm. The SEM image of Zn(II) complex seemed heterogeneous surfaced with average particle size 250 nm.

Antibacterial and antifungal activity: Antimicrobial activity was carried out by the cup-plate method [40,41]. The ligand (5-MeTAMB) and its Ni(II), Cu(II) and Zn(II) complexes have been tested for their antibacterial and antifungal activity at 1 mg/mL concentration, DMSO is used as solvent. The results of antimicrobial activity have been statistical presented in Fig. 7, which showed that the ligand and Zn(II) complex of showed less activity against *S. aureus* and *E. coli* when compared with that of standard drug streptomycin. The Cu(II) complex of showed good activity while Ni(II) complex of exhibited moderate activity against *S. aureus*, when compared with that of standard drug streptomycin.

The results of the antifungal activity of Ni(II) complex showed good activity against *A. niger* when compared with standard drug fluconazole at the same concentration as that of the test compound and DMSO is used as solvent. The ligand and Cu(II) and Zn(II) complexes of showed less activity against *A. niger* when compared with standard drug fluconazole.

TABLE-7
POWDER X-RAY DIFFRACTION DATA OF LIGAND (5-MeTAMB) AND ITS METAL(II) COMPLEXES

Compound	No.	$2\theta_{observed}$ (°)	$d_{observed}$ (Å)	I/I_o (%)	FWHM	Crystallite size (nm)	Lattice strain
5-MeTAMB	1	31.7832	2.821000	100	0.14290	60.77	0.0022
	2	45.4763	1.994000	15	0.20500	63.33	0.0015
	3	66.2563	1.409000	8	0.15530	63.82	0.0010
Ni(II) complex	1	31.5914	2.82982	100	0.86000	10.03	0.0133
	2	19.2152	4.61535	79	0.18000	46.76	0.0046
	3	45.3805	1.99689	53	0.66000	13.63	0.0069
Cu(II) complex	1	16.1826	5.47279	100	0.35990	23.30	0.0110
	2	32.2991	2.76941	99	0.52290	16.53	0.0079
	3	39.6701	2.27017	77	0.52000	16.97	0.0063
Zn(II) complex	1	23.0609	3.85364	100	0.12760	66.4	0.0027
	2	6.7101	13.16230	91	0.21530	38.62	0.0160
	3	33.3962	68090.2	36	0.12750	67.97	0.0019

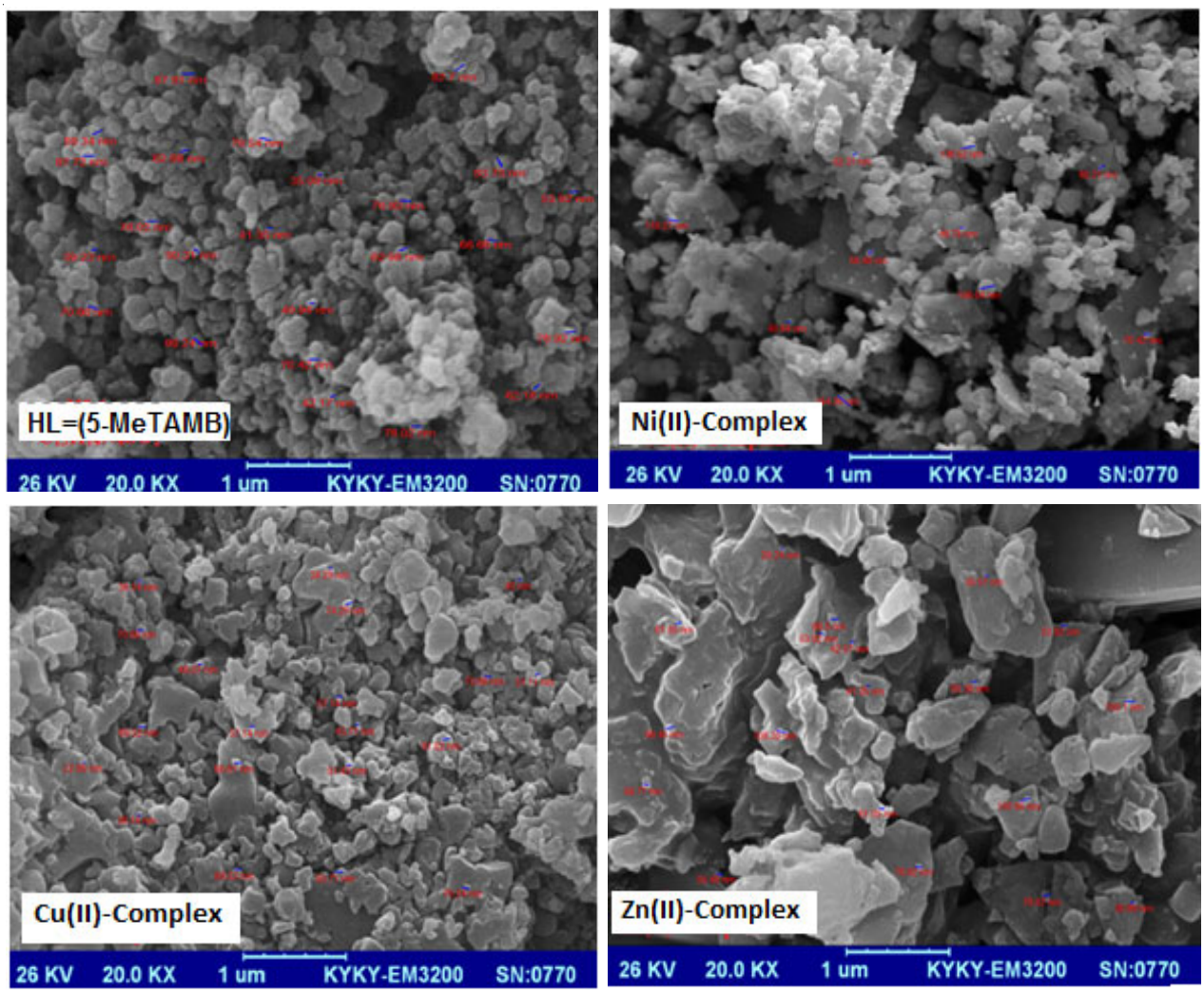

Fig. 6. SEM images of ligand (5-MeTAMB) and its prepared metal complexes

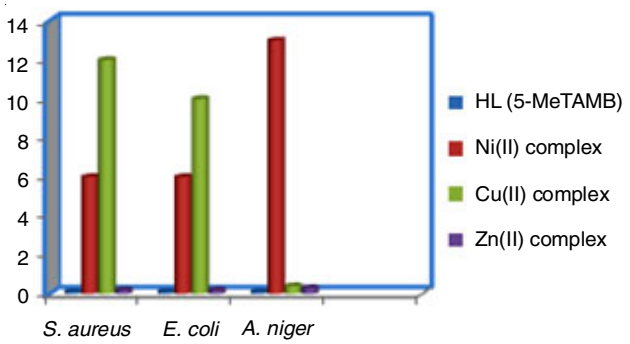

Fig. 7. Statistical representation for biological activity of ligand (5-MeTAMB) and its metal complexes

***in vitro* Cytotoxicity assays:** Chemotherapy is the major approach for both localized and metastasized cancer [42,43]. Therefore, the ligand (5-MeTAMB) and its Cu(II) complex were screened for their *in vitro* cytotoxicity and growth inhibitory activities against human tumor cell line breast cancer cell line MCF-7.

The relation between the biological activity of the cancerous line cell of the breast MCF-7 and normal line cells of the breast WRL and the concentration of the ligand and its complex with Cu(II) ion. It is observed that the inhibition of the ligand (5-MeTAMB) differs with difference of cell line where the number of the remaining living cells after the reaction with Cu(II) complex. The ligand for is observed that the highest ratio of the inhibition for the cancerous cell line of the breast MCF-7 is 47.47 % whereas the ratio of the normal cell line WRL is 77.67 % for the living cells when concentration of 200 μg mL^{-1} and this indicates that Cu(II) complex has a higher efficiency than the ligand inhibiting the growth of cancerous cells Cu(II) complex is observed that the highest ratio of the inhibition for the cancerous cell line of the breast MCF-7 is 47.5 % whereas the ratio of the normal cell line WRL is 92.4 % for the living cells when concentration issued 100 μg mL^{-1}. The screening results are given in Table-8. The reason behind this inhibition of the growth of cancer cell is that the ligand and Cu(II) complex include thiazole ring which has a high efficiency in inhibiting or stopping the growth of cancer cells. Moreover, increasing the efficiency in inhibiting the growth of cancer cells by using Cu(II) complex is more than that in the ligand because it includes two thiazole rings [44].

The cytotoxicity of the tested compounds was expressed by IC_{50} median growth inhibitory concentration which required producing 50 % cytotoxic effect against cancer cells after 24 h exposure to tested compounds. The screening results shown in Figs. 8 and 9. It is evident that for MCF-7 cells, the tested (5-MeTAMB) and its Cu(II) complex showed anticancer

TABLE-8
EFFECT OF LIGAND (5-MeTAMB) AND Cu(II) COMPLEX ON BREAST CANCEROUS CELLS MCF7 VAIBILITY AND COMPARISON WITH NATURAL CELLS LINE (WRL-68) FOR SAME CONCENTRATION USING 24 h MTT TEST AT 37 °C

Conc. (μg mL^{-1})	5-MeTAMB				Cu(II) complex			
	Cancerous line cells of breast MCF7		Normal line cells of breast WRI-68		Cancerous line cells of breast MCF7		Normal line cells of breast WRI-68	
	Mean	SD	Mean	SD	Mean	SD	Mean	SD
6.25	–	–	47.33	44.3	98.6	1.73	73.9	12.10
12.5	100.00	5.1	30.36	15.7	99.9	1.14	83.2	12.48
25	97.62	12.2	53.58	31.4	100.0	6.09	78.8	13.89
50	90.66	16.9	100.00	51.5	84.6	7.59	100.0	31.80
100	84.27	15.0	61.61	82.8	47.5	9.80	92.4	38.98
200	47.47	3.4	77.67	55.1	33.0	1.70	54.1	8.59
400	4.74×10^{-15}	4.7	1.26×10^{-13}	65.9	6.5×10^{-15}	7.74	5.2×10^{-14}	21.42

activity with IC_{50} values that ranged of concentration from 6.25 to 400 μg mL^{-1}. *in vitro* Cytotoxicity of the ligand (5-MeTAMB), on human cell lines MCF-7, (HL) showed cytotoxicity against cancer cell line with IC_{50} = 183.5 μg/mL; WRI-68 IC_{50} = 210.2 μg/mL, while Cu(II) complex showed selective cytotoxicity against cancer cell line with IC_{50} = 109.9 μg/mL; WRI-68 IC_{50} = 205.0 μg/mL. The results showed that the type of compound plays an important role in the rate of inhibition of the growth of cells of cancerous and natural lines.

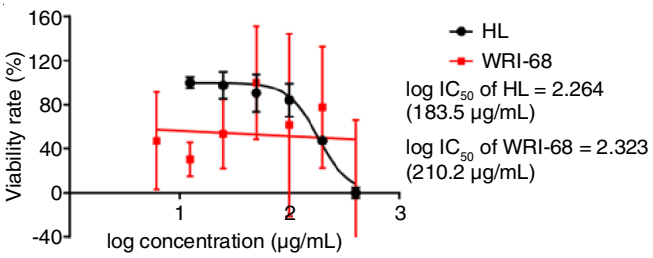

Fig. 8. Anticancer activity data ligand (5-MeTAMB) against human cancer cell lines

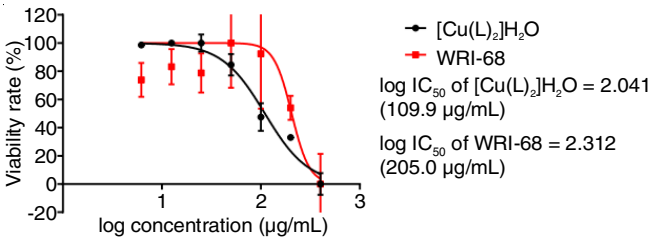

Fig. 9. Anticancer activity data of Cu(II) complex against human cancer cell lines

Conclusion

In this article we reported a synthesis and spectral identification of new azo dye ligand (5-MeTAMB) and its metal complexes with Ni(II), Cu(II) and Zn(II) ions. The structure of ligand and its metal complexes was confirmed by elemental analysis and spectroscopic techniques. The geometry proposed for all metal complexes is octahedral structure (Fig. 10) and is not effected by air, light and a moisture. It suggest high stability. The ligand and its metal complexes are found to have biological activities toward antibacterial and antifungal. The biological activity also conducted cells viability and cytotoxicity assays on ligand (5-MeTAMB) and its Cu(II) complex by using the lines of cancerous barest cells, of the type MCF7 and compared

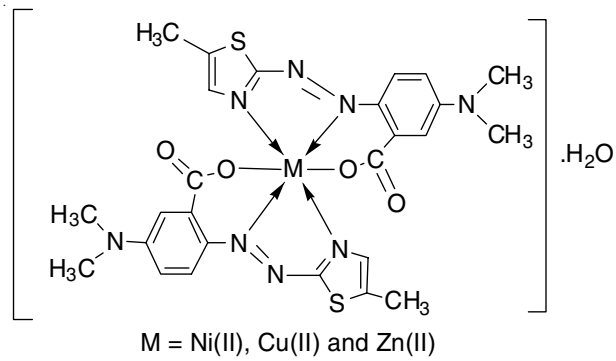

Fig. 10. Proposed structural formula of M(II) complexes

with line of the ordinary cells, through tests conducted to identify the possibility of using the ligand and Cu(II) complex as drugs to treat some cancerous diseases that affect humans.

REFERENCES

1. K.A. Ahmed, H.M. Elhennawy and M.A. Elkashouti, *Res. J. Chem. Sci.*, **2**, 14 (2012).
2. L.-H. Ahlström, C.S. Eskilsson and E. Björklund, *TrAC Trends Anal. Chem.*, **24**, 49 (2005); https://doi.org/10.1016/j.trac.2004.09.004.
3. V.A. Lemos, E.S. Santos, M.S. Santos and R.T. Yamaki, *Microchim. Acta*, **158**, 189 (2007); https://doi.org/10.1007/s00604-006-0704-9.
4. K. Bredereck, *Dyes Pigments*, **21**, 23 (1993); https://doi.org/10.1016/0143-7208(93)85003-I.
5. G.M. Malik and S.K. Zadafiva, *Der Chem. Sinica*, **1**, 15 (2010).
6. L.-H. Ahlström, C. Sparr Eskilsson and E. Björklund, *Trends Analyt. Chem.*, **24**, 49 (2005); https://doi.org/10.1016/j.trac.2004.09.004.
7. A. Khosravi, S. Moradian, K. Gharanjig and F.A. Taromi, *Dyes Pigments*, **69**, 79 (2006); https://doi.org/10.1016/j.dyepig.2005.02.007.
8. A.A. Zuhair, K.J. Al-Adilee and T. Zianab, *Int. Res. J. Pure Appl. Chem.*, **8,** 33 (2015)
9. X. Fan, C. Zhu and G. Zhang, *Analyst*, **123**, 109 (1998); https://doi.org/10.1039/a705268e.
10. K. Syrmanova, E. Negim, J. Kaldybekova and A.M. Tuleuov, *Orient. J. Chem.*, **32**, 01 (2016); https://doi.org/10.13005/ojc/320101.
11. U. Parimi and L. Pappu, *Int. J. Pharm. Pharm. Sci.*, **4**, 523 (1998).
12. G. Giorgioni, B. Accorroni, A. Di Stefano, G. Marucci, A. Siniscalchi and F. Claudi, *Med. Chem. Res.*, **14**, 57 (2005); https://doi.org/10.1007/s00044-005-0125-z.
13. T.D. Bradshaw, M.F. Stevens and A.D. Westwell, *Curr. Med. Chem.*, **8**, 203 (2001); https://doi.org/10.2174/0929867013373714.

14. P. Venkatesh and S.N. Pandeya, *Int. J. Chem. Tech. Res.*, **1**, 1354 (2002).
15. K.C. Keerthi, J. Keshavayya, T. Ragesh and S.K. Peethampar, *Int. J. Pharm. Pharm. Sci.*, **5**, 296 (2013).
16. M.R. Yazdanbakhsh, H. Yousefi, M. Mamaghani, E.O. Moradi, M. Rassa, H. Pouramir and M. Bagheri, *J. Mol. Liq.*, **6**, 21 (2012); https://doi.org/10.1016/j.molliq.2012.03.003.
17. M. Amir, S. Alamkhan and S.K. Peethampar, *J. Indian Chem. Soc.*, **79**, 280 (2002).
18. K.J. Al-Adilee and H.M. Hessoon, *J. Chem. Pharm. Res.*, **7**, 89 (2015).
19. K.J. Al-Adilee and S.H. Jawad, *J. Global Pharma Technol.*, (In Press).
20. K.J. Al-Adilee and D.Y. Fanfon, *J. Chem. Chem. Eng.*, **6**, 1016 (2012); https://doi.org/10.17265/1934-7375/2012.11.011.
21. X. Fan, C. Zhu and G. Zhang, *Analyst*, **123**, 109 (1998); https://doi.org/10.1039/a705268e.
22. G.P. Hildebrand and C.N. Reilley, *Anal. Chem.*, **29**, 258 (1957); https://doi.org/10.1021/ac60122a025.
23. K.J. Al-Adilee, H.A.H. Al-Shamsi and M.N. Dawood, *Res. J. Pharm. Biol. Chem. Sci.*, **7**, 2882 (2016).
24. K.J. Al-Adilee and S. Adnan, *Orient. J. Chem.*, **33**, 1815 (2017); https://doi.org/10.13005/ojc/330426.
25. A. Mostafa, N. El-Ghossein, G.B. Cieslinski and H.S. Bazzi, *J. Mol. Struct.*, **1054-1055**, 199 (2013); https://doi.org/10.1016/j.molstruc.2013.09.007.
26. K.J. Al-Adilee, *Asian J. Chem.*, **24**, 5419 (2012).
27. W.C. Vosburgh and G.R. Cooper, *J. Am. Chem. Soc.*, **63**, 437 (1941); https://doi.org/10.1021/ja01847a025.
28. E. Mercer, W. Peterson and B. Jordan, *J. Inorg. Nucl. Chem.*, **34**, 3290 (1972); https://doi.org/10.1016/0022-1902(72)80139-8.
29 K.J. Al-Adilee, A.K. Abass and A.M. Taher, *J. Mol. Struct.*, **1108**, 378 (2016); https://doi.org/10.1016/j.molstruc.2015.11.038.
30. S. Chandra, M. Tyagi and K. Sharma, *J. Iran. Chem. Soc.*, **6**, 310 (2009); https://doi.org/10.1007/BF03245839.
31. K.J. Al-Adilee and B.A. Hatem, *J. Adv. Chem.*, **11**, 3412 (2015); https://doi.org/10.24297/jac.v11i3.870.
32. K.J. Al-Adilee, K.A. Abedalrazaq and Z.M. Al-Hamdiny, *Asian J. Chem.*, **25**, 10475 (2013); https://doi.org/10.14233/ajchem.2013.15735.
33. V. Bankova, *Chem. Cent. J.*, **1**, 1 (2007); https://doi.org/10.1186/1752-153X-1-1.
34. H. Alshamsi, K. Al-Adilee and S.A. Jaber, *Orient. J. Chem.*, **31**, 809 (2015); https://doi.org/10.13005/ojc/310223.
35. M.B. Halli, K. Mallikarjun and S.S. Suryakant, *J. Chem. Pharm. Res.*, **7**, 1797 (2015).
36. H.A. Habeeb, K.J. Al-Adilee and S.A. Jaber, *J. Chem. Mater. Res.*, **6**, 69 (2014).
37. M.A. Neelakantan, S.S. Marriappan, J. Dharmaraja, T. Jeyakumar and K. Muthukumaran, *Spectrochim. Acta Part A: Mol. Biomol. Spectrosc.*, **71**, 628 (2008); https://doi.org/10.1016/j.saa.2008.01.023.
38. C. Anitha, S. Sumathi, P. Tharmaraj and C.D. Sheela, *Int. J. Inorg. Chem.*, **Article ID 493942** (2011); https://doi.org/10.1155/2011/493942.
39 K. Al-Adilee and H.A.K. Kyhoiesh, *J. Mol. Struct.*, **1137**, 160 (2017); https://doi.org/10.1016/j.molstruc.2017.01.054.
40. C.M. Harris and D.B. Kell, *Biosensors,* **1**, 17 (1985); https://doi.org/10.1016/0265-928X(85)85005-7.
41. K. Mazumdar, N.K. Dutta, K.A. Kumar and S.G. Dastidar, *Biol. Pharm. Bull.*, **28**, 713 (2005); https://doi.org/10.1248/bpb.28.713.
42. Shamsuzzaman, A.M. Dar, H. Khanam and M.A. Gatoo, *Arab. J. Chem.*, **7**, 461 (2014); https://doi.org/10.1016/j.arabjc.2013.06.027.
43. W.-X. Cai, A.-L. Liu, Z.-M. Li, W.-L. Dong, X.-H. Liu and N.-B. Sun, *Appl. Sci.*, **6**, 8 (2016); https://doi.org/10.3390/app6010008.
44. S.L. Yan, M.-Y. Yang, Z.-H. Sun, L.-J. Min, C.X. Tan, J.-Q. Weng, H.-K. Wu and X.-H. Liu, *Lett. Drug Des. Discov.*, **11**, 940 (2014); https://doi.org/10.2174/15701808116661404232221 41.